Radiopharmaceuticals Hot Paper

International Edition: DOI: 10.1002/anie.201709532
German Edition: DOI: 10.1002/ange.201709532

An Eighteen-Membered Macrocyclic Ligand for Actinium-225 Targeted Alpha Therapy

Nikki A. Thiele, Victoria Brown, James M. Kelly, Alejandro Amor-Coarasa, Una Jermilova, Samantha N. MacMillan, Anastasia Nikolopoulou, Shashikanth Ponnala, Caterina F. Ramogida, Andrew K. H. Robertson, Cristina Rodríguez-Rodríguez, Paul Schaffer, Clarence Williams, Jr., John W. Babich, Valery Radchenko, and Justin J. Wilson**

Abstract: *The 18-membered macrocycle H_2macropa was investigated for ^{225}Ac chelation in targeted alpha therapy (TAT). Radiolabeling studies showed that macropa, at submicromolar concentration, complexed all ^{225}Ac (26 kBq) in 5 min at RT. $[^{225}Ac(macropa)]^+$ remained intact over 7 to 8 days when challenged with either excess La^{3+} ions or human serum, and did not accumulate in any organ after 5 h in healthy mice. A bifunctional analogue, macropa-NCS, was conjugated to trastuzumab as well as to the prostate-specific membrane antigen-targeting compound RPS-070. Both constructs rapidly radiolabeled ^{225}Ac in just minutes at RT, and macropa-Tmab retained >99% of its ^{225}Ac in human serum after 7 days. In LNCaP xenograft mice, ^{225}Ac-macropa-RPS-070 was selectively targeted to tumors and did not release free ^{225}Ac over 96 h. These findings establish macropa to be a highly promising ligand for ^{225}Ac chelation that will facilitate the clinical development of ^{225}Ac TAT for the treatment of soft-tissue metastases.*

Radium-223 (^{223}Ra) is the first therapeutic α-emitting radionuclide to be approved for clinical use in cancer patients. Administered as $^{223}RaCl_2$, it has been employed in the treatment of metastatic castration-resistant prostate cancer since 2013.[1] The osteophilic nature and high-energy α-particle emanations, respectively, of $^{223}Ra^{2+}$ ions are effective for targeting and eradicating bone metastases originating from this disease.[2] To more generally harness the therapeutic potential of α-particles for soft-tissue metastases, the strategy of targeted alpha-particle therapy (TAT) has emerged,[3,4] whereby lethal α-emitting radionuclides are conjugated to tumor-targeting vectors using bifunctional chelators[5] to selectively deliver cytotoxic α radiation to cancer cells (Figure 1a).

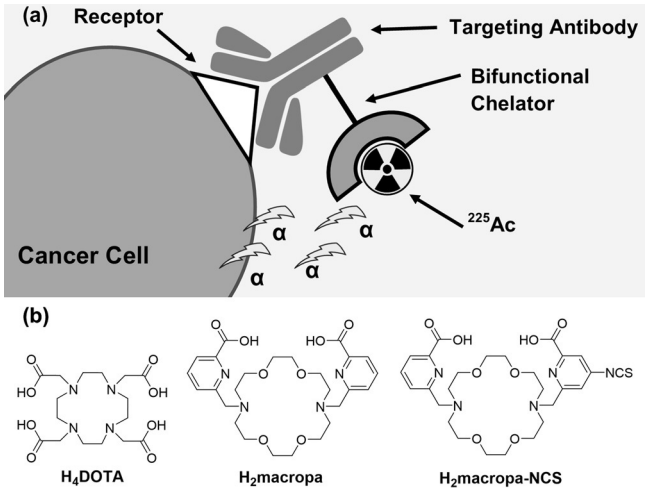

Figure 1. a) Schematic diagram depicting the concept of targeted alpha therapy using ^{225}Ac. b) Structures of the ligands discussed in this work.

Among the suitable radionuclides for such an application, actinium-225 (^{225}Ac) is highly promising for use in TAT owing to its long 10-day half-life that is compatible with antibody-based targeting vectors and four high-energy α-emissions that are extremely lethal to cells.[6–10] A key challenge for the implementation of ^{225}Ac TAT is the lack of a suitable bifunctional chelator that can rapidly bind the Ac^{3+} ion and stably retain it in vivo.[11–14] Although a highly promising bispidine-based chelator has recently been disclosed,[15] the 12-membered tetraaza macrocycle H_4DOTA (Figure 1b) is currently the state of the art for the chelation of the $^{225}Ac^{3+}$ ion.[7,12,16] However, the thermodynamic stabilities of complexes of H_4DOTA decrease as the ionic radius of the metal ion increases,[17,18] thus indicating that this ligand is not optimal for chelation of the Ac^{3+} ion, the largest +3 ion in the periodic table.[19] Furthermore, the ^{225}Ac-radiolabeling kinetics of this ligand are slow (see below), thus necessitating the

[*] Dr. N. A. Thiele, Dr. S. N. MacMillan, Prof. J. J. Wilson
Chemistry and Chemical Biology, Cornell University
Ithaca, NY 14853 (USA)
E-mail: jjw275@cornell.edu

V. Brown, U. Jermilova, Dr. C. F. Ramogida, A. K. H. Robertson, Dr. P. Schaffer, Dr. V. Radchenko
Life Science Division, TRIUMF
Vancouver, BC V6T 2A3 (Canada)
E-mail: vradchenko@triumf.ca

Dr. J. M. Kelly, Dr. A. Amor-Coarasa, Dr. A. Nikolopoulou, Dr. S. Ponnala, C. Williams Jr., Prof. J. W. Babich
Radiology, Weill Cornell Medicine
New York, NY 10065 (USA)

Dr. C. Rodríguez-Rodríguez
Fac. of Pharmaceutical Sciences, Dept. of Physics and Astronomy and Centre for Comparative Medicine, University of British Columbia
Vancouver BC V6T 1W5 (Canada)

Supporting information and the ORCID identification number(s) for the author(s) of this article can be found under: https://doi.org/10.1002/anie.201709532.

application of heat if short labeling times are required.[16,20–22] In our search for an improved ^{225}Ac chelator, we investigated *N*,*N*′-bis[(6-carboxy-2-pyridil)methyl]-4,13-diaza-18-crown-6, herein called H_2macropa (Figure 1b), an expanded 18-membered macrocyclic ligand that can optimally accommodate the large 1.12 Å ionic radius (CN 6)[19] of Ac^{3+}. Our studies have revealed H_2macropa to be superior to H_4DOTA for the rapid chelation of ^{225}Ac. Additionally, we report the synthesis of the first bifunctional analogue of H_2macropa, H_2macropa-NCS (Figure 1b), which exhibits facile and stable chelation of ^{225}Ac after conjugation to both antibody and small-molecule tumor-targeting vectors.

H_2macropa was synthesized according to published procedures[23,24] and characterized by conventional techniques, including X-ray crystallography (see Figure S1, and Tables S1 and S2 in the Supporting Information). Previous studies have shown that macropa, for which the thermodynamic affinity for the whole lanthanide series was evaluated, is selective for the larger metal ions La^{3+}, Pb^{2+}, and Am^{3+} over the smaller Lu^{3+}, Ca^{2+}, and Cm^{3+} ions.[24–26] Based on this selectivity pattern, we hypothesized that macropa would effectively chelate the large Ac^{3+} ion. Before assessing its Ac-chelation properties, complex formation was evaluated in situ between macropa and cold La^{3+} and Lu^{3+} ions. In these studies, La^{3+} was used as a non-radioactive surrogate for $^{225}Ac^{3+}$ because it is chemically similar albeit slightly smaller (1.03 Å, CN 6).[19] Complexation of the smaller Lu^{3+} ion (0.861 Å, CN 6)[19] by macropa was investigated to probe its size selectivity. La^{3+} and Lu^{3+} titrations confirmed the high affinity of these metal ions for macropa at pH 7.4 (see Figure S2), consistent with the previously measured stability constants ($\log K_{LaL} = 14.99$, $\log K_{LuL} = 8.25$).[24] The kinetic inertness of these complexes formed in situ was investigated by challenging them with an excess of either ethylenediaminetetraacetic acid (EDTA) or diethylenetriaminepentaacetic acid (DTPA), chelators which have a higher thermodynamic affinity than macropa for Lu^{3+} and La^{3+} ions ($\log K_{LuEDTA} = 19.80$ and $\log K_{LaDTPA} = 19.48$).[27] The Lu^{3+} ion was transchelated within 1 minute upon the addition of only 10 equivalents of EDTA, whereas the La^{3+} complex remained intact for up to 21 days in the presence of 1000 equivalents of DTPA (see Figure S3). These results demonstrate that, despite a strong thermodynamic preference for DTPA to transchelate La^{3+}, the high level of kinetic inertness of the macropa complex inhibits this process on a detectable time scale.

The preference of macropa for the larger La^{3+} ion over the smaller Lu^{3+} ion is further manifested in the structural architectures of the corresponding complexes. The La^{3+} and Lu^{3+} complexes of macropa were isolated and characterized (see Figures S4–S14), and their solid-state structures were elucidated by X-ray crystallography (Figure 2; see Tables S1, S3, and S4). As observed in the previously reported structures of macropa complexes of Gd^{3+} and Yb^{3+},[24] the La^{3+} and Lu^{3+} ions reside above the 18-membered macrocycle, and the two picolinate arms are positioned on the same side of the macrocycle. The coordination sphere of the Lu^{3+} ion is satisfied by the ten donors of macropa with both picolinate arms deprotonated. In contrast, the larger La^{3+} ion forms an 11-coordinate complex by the incorporation of an inner-sphere water molecule which penetrates the macrocycle. This structural motif was also observed in a crystal structure of the La^{3+} complex of a related ligand, ppa18c6.[28] The ability of macropa to form stable 11-coordinate complexes is of particular significance because recent EXAFS studies have demonstrated that Ac^{3+} prefers a coordination number of 11 in aqueous solutions.[29,30] An interesting difference between the La^{3+} and Lu^{3+} structures is that one of the picolinate arms in the La^{3+} complex is protonated, thus giving a cationic formula of $[La(Hmacropa)(H_2O)]^{2+}$. This hydrogen atom was located directly on the difference Fourier map and refined semi-freely. A close intermolecular contact (2.468 Å) between O6 and O8 in neighboring molecules in the crystal lattice also supports the presence of a hydrogen atom, which mediates this short hydrogen bond. Similarly, protonation of one picolinate arm has been observed in the crystal structure of the Zn^{2+} complex of H_2bp12c4, a 12-membered analogue of H_2macropa.[31] Consistent with the larger ionic radius of La^{3+}, the La-donor distances are on average approximately 0.30 Å longer than those in the Lu^{3+} complex. Notably, the La^{3+} ion is situated symmetrically within the macrocycle, whereas the Lu^{3+} ion resides to one side of the macrocycle, as evidenced by the disparate Lu-N1 and Lu-N2 distances of 2.810(5) versus 2.909(6) Å, respectively. The asymmetric situation of the smaller Lu^{3+} ion within macropa is most likely a factor that contributes to its decreased stability.

Based on the promising results obtained with the large La^{3+} ion, we pursued macropa for the chelation of the even larger, radioactive $^{225}Ac^{3+}$ ion and compared it to the current gold standard, DOTA (see Figure S15a and Tables S5–8).

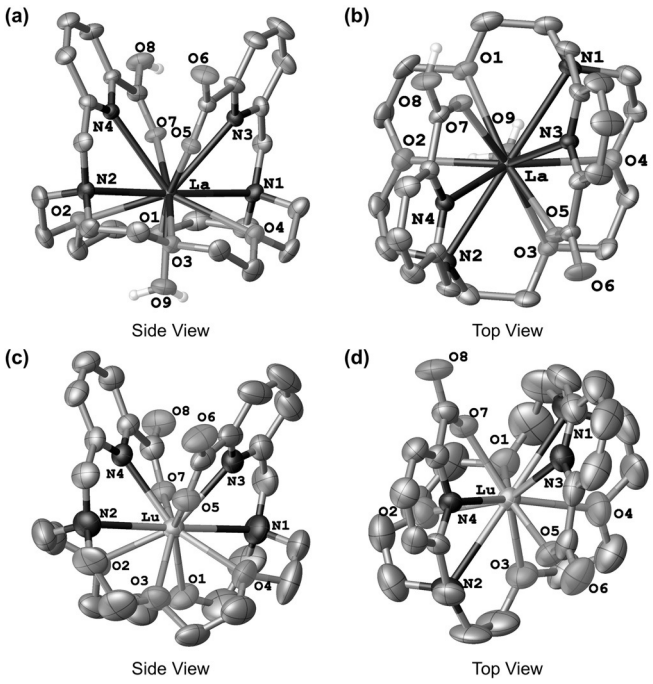

Figure 2. X-ray crystal structures of $[La(Hmacropa)(H_2O)]\cdot(ClO_4)_2$ (a,b) and $[Lu(macropa)]\cdot ClO_4\cdot DMF$ (c,d). Ellipsoids are drawn at the 50% probability level. Counteranions, hydrogen atoms attached to carbon centers, and outer-sphere solvent molecules are omitted for clarity. Interatomic distances [Å] are in the Supporting Information.

Both ligands (59 μM) were incubated with ^{225}Ac (26 kBq) in 0.15 M NH_4OAc buffer at pH 5.5–6, and the complexation reaction was monitored by radio-TLC (see Figure S16) after 5 minutes. Remarkably, macropa complexed all the ^{225}Ac after merely 5 minutes at room temperature, whereas DOTA only complexed 10% under these conditions. At this ligand concentration, complete radiolabeling of DOTA could only be achieved at 80 °C, a temperature incompatible with antibodies and most proteins. At 100-fold lower concentration (0.59 μM) of macropa, a L:M ratio of only 1800, radiolabeling was still complete at room temperature in 5 minutes. At this concentration, DOTA failed to complex ^{225}Ac even at 80 °C. At a 0.0059 μM concentration, neither ligand could chelate ^{225}Ac. Taken together, these studies reveal macropa to exhibit excellent radiolabeling kinetics at ambient temperature and submicromolar ligand concentration, conditions under which DOTA fails. We postulate that the expanded macrocyclic core of macropa is better matched to the large size of the Ac^{3+} ion than is the smaller macrocyclic core of DOTA. This optimal fit may minimize the activation energy associated with the reorganization of macropa into the proper conformation for Ac^{3+} binding, thus leading to the superior radiolabeling kinetics of macropa observed here.

The long half-life of ^{225}Ac necessitates its stable complex retention in vivo to avoid off-target damage to normal tissues arising from the release of free $^{225}Ac^{3+}$. As such, the stability of ^{225}Ac complexes against transmetalation and transchelation needs to be high. To test its kinetic inertness, we first challenged $[^{225}Ac(macropa)]^+$ with La^{3+} because of the established high affinity of macropa for this metal ion. A 50-fold excess of La^{3+}, with respect to ligand concentration, was added to ^{225}Ac-radiolabeled solutions of macropa (0.59 μM) at room temperature. Over seven days, 98% of the ^{225}Ac complex remained intact as determined by radio-TLC, thus signifying that an excess of La^{3+} is unable to displace $^{225}Ac^{3+}$ (see Figure S15b). Because intravenous administration is the primary delivery route for TAT conjugates, the stability of $[^{225}Ac(macropa)]^+$ in human serum was also evaluated by radio-TLC. This study revealed that $^{225}Ac^{3+}$ remains complexed by macropa for at least 8 days (see Figure S15b). The impressive stability exhibited by $[^{225}Ac(macropa)]^+$ was similar to that of $[^{225}Ac(DOTA)]^-$ in either the presence of excess La^{3+} or in human serum (see Table S9; control study in Table S10), which was also stable under these conditions. It is worth noting, however, that $[^{225}Ac(DOTA)]^-$ was prepared with a 100-fold higher concentration (59 μM) of ligand compared to $[^{225}Ac(macropa)]^+$ (0.59 μM) for these stability studies, thus giving rise to higher quantities of free ligand in solution to stabilize the complex. Importantly, these studies signify that the improved radiolabeling kinetics of macropa over DOTA do not come at the cost of kinetic inertness of the resulting $[^{225}Ac(macropa)]^+$ complex.

These encouraging results prompted us to evaluate the in vivo stability of $[^{225}Ac(macropa)]^+$ by comparing its biodistribution to those of $^{225}Ac(NO_3)_3$ and $[^{225}Ac(DOTA)]^-$. C57BL/6 mice were injected in the tail vein with 10–50 kBq of each radiometal complex and were sacrificed after either 15 minutes, 1 hour, or 5 hours. The amount of ^{225}Ac retained in each organ was quantified by γ counting and reported as the percent of injected dose per gram of tissue (% ID g^{-1}). The results of these studies are compiled in Tables S11–S13. Inadequate stability of an ^{225}Ac complex leading to the loss of a radioisotope in vivo is manifested by the accumulation of ^{225}Ac in the liver, spleen, and bone of mice.[11,12,32] As expected, the biodistribution profile of uncomplexed $^{225}Ac(NO_3)_3$ (Figure 3a) reveals slow blood clearance and excretion, coupled to large accumulation in the liver and spleen. The biodistribution profile of $[^{225}Ac(macropa)]^+$ (Figure 3b) differs markedly from that of $^{225}Ac(NO_3)_3$. $[^{225}Ac(macropa)]^+$ was rapidly cleared from mice, with very little activity measured in blood by 1 hour post injection. Most of the injected dose was renally excreted and subsequently detected in the urine, explaining the moderate kidney and bladder uptake of $[^{225}Ac(macropa)]^+$ observed in mice at 15 minutes and 1 hour post injection. Of significance, $[^{225}Ac(macropa)]^+$ did not accumulate in any organ over the time course of the study, thus indicating that the complex does not release free $^{225}Ac^{3+}$ in vivo. Its biodistribution profile was similar to that of $[^{225}Ac(DOTA)]^-$ (Figure 3c), which has been previously shown to retain $^{225}Ac^{3+}$ in vivo.[7] Notably, $[^{225}Ac(DOTA)]^-$ appeared to clear more rapidly through the urine and was taken up to a lesser extent in the thyroid. These differences may arise in part because of the opposite charges of the complexes. Collectively, the results of these biodistribution studies demonstrate that $[^{225}Ac(macropa)]^+$ is highly stable in vivo.

Armed with these exciting results that demonstrate macropa to be an exceptional chelator for ^{225}Ac, we next

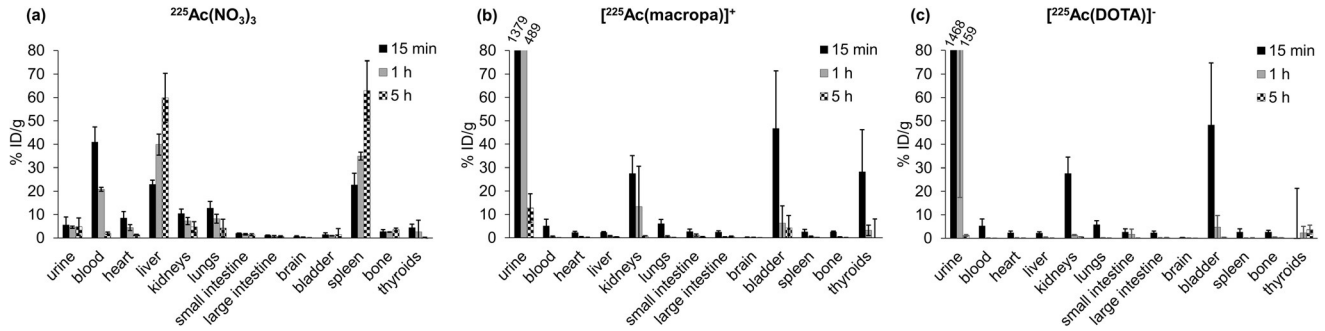

Figure 3. Distribution of a) $^{225}Ac(NO_3)_3$, b) $[^{225}Ac(macropa)]^+$, and c) $[^{225}Ac(DOTA)]^-$ for select organs following intravenous injection in mice. Adult C57BL/6 mice were sacrificed 15 min, 1 h, or 5 h post injection. Values for each time point are given as mean % ID g^{-1} ± 1 SD.

sought to incorporate this ligand into tumor-targeting constructs. To facilitate its conjugation, a reactive isothiocyanate functional group was installed onto one of the picolinate arms of macropa to give the novel bifunctional ligand macropa-NCS (Figure 1b). The isothiocyanate reacts with amine functional groups, such as those found on lysine residues, of potential targeting vectors to form a thiourea linker. Macropa-NCS was synthesized over eight steps (see Scheme S1) and characterized by conventional techniques (see Figures S17–S53). It was found to be substantially more reactive than *p*-SCN-Bn-DOTA, a widely used bifunctional analogue of DOTA, based on hydrolysis experiments in pH 9 $NaHCO_3$ buffer (Figures S54 and S55). A model conjugate, macropa-$NHC(S)NHCH_3$, was then isolated from the reaction of macropa-NCS with methylamine. The conjugate retained its high affinity for La^{3+} and the resulting complex was kinetically inert in a DTPA challenge (see Figure S56). These results suggest that a thiourea linker directly attached to one chelating picolinate arm of macropa does not significantly alter the ligand's affinity for large metal ions.

The bifunctional ligand was subsequently conjugated to trastuzumab (Tmab), an FDA-approved monoclonal antibody which targets the human epidermal growth factor receptor 2 (HER2) in breast and other cancers.[33] With a biological half-life of several weeks,[34,35] Tmab is an ideal vector to shuttle the long-lived ^{225}Ac radionuclide to tumor cells. For comparison, *p*-SCN-Bn-DOTA was also conjugated to Tmab. The conjugates were analyzed by MALDI-ToF mass spectrometry to determine the average number of ligands per antibody, which was 2.4 for macropa-Tmab and 4.2 for DOTA-Tmab (see Figures S57–S59). In radiolabeling experiments, macropa-Tmab complexed ^{225}Ac in greater than 99% RCY after just 5 minutes at room temperature and pH 5 using 25–100 μg of antibody conjugate (see Table S14). However, DOTA-Tmab (100 μg) was unable to chelate ^{225}Ac at room temperature, even after 4 hours (see Table S15; control study in Table S16). ^{225}Ac-macropa-Tmab displayed excellent stability in human serum at 37 °C. After 7 days, greater than 99% of the complex remained intact (see Table S17). Together, these results highlight the efficacy of macropa as a chelator for ^{225}Ac in antibody constructs. We anticipate that macropa will facilitate the further development of ^{225}Ac TAT by enabling facile single-step formation of radiolabeled antibodies with high specific activity at room temperature.

Work in our laboratories has also focused on the development of dual-targeting small-molecule constructs for the treatment of prostate cancer.[36] These constructs bear a glutamate-urea-lysine moiety which inhibits the prostate-specific membrane antigen (PSMA),[37–41] a membrane-bound glycoprotein which is overexpressed in prostate cancer cells.[42] An albumin-binding functional group, in this case iodophenyl, is also a critical component of these compounds and prolongs their circulation half-life.[43,44] One such PSMA/albumin dual-targeting small molecule, RPS-070, was conjugated to macropa-NCS and characterized (Figure 4a; see Scheme S2). Radiolabeling of macropa-RPS-070 with ^{225}Ac proceeded within 20 minutes at room temperature and pH 5–5.5 to give a RCY of 98%. ^{225}Ac-macropa-RPS-070 (85–95 kBq) was then injected into LNCaP (prostate cancer) tumor xenograft-bearing mice, and the biodistribution of the complex was determined at 4, 24, and 96 hours post injection (see Table S18). As shown in Figure 4b, ^{225}Ac-macropa-RPS-070 was rapidly cleared from the blood and primarily distributed to the kidneys and tumor (52 ± 16% ID g^{-1} and 13 ± 3% ID g^{-1}, respectively, at 4 h post injection). After 4 hours, most of the activity cleared from the kidneys and gradual tumor washout was observed. Importantly, the complex exhibited negligible uptake by other organs (< 1% ID g^{-1} at 96 h post injection) and did not amass in any organ over time. The activity that cleared from the tumor within 4–96 hours remained chelated by macropa-RPS-070, as evidenced by the lack of accumulation of ^{225}Ac in the liver, spleen, and bone of mice during this time. These results are significant because they demonstrate that macropa-RPS-070 can stably retain ^{225}Ac in vivo over several days and that the construct can be selectively targeted to tumors. Efforts are currently underway to optimize the pharmacokinetics of these dual-targeted constructs.

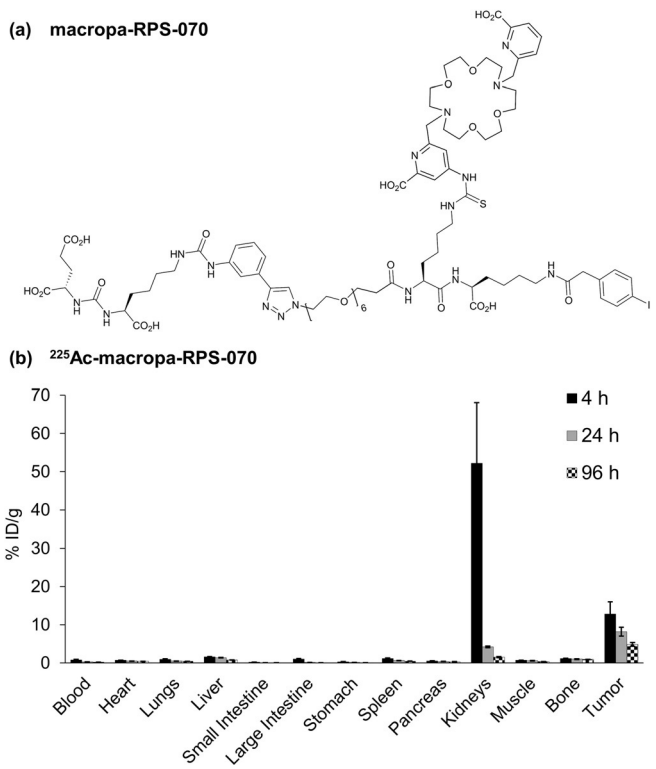

Figure 4. a) Structure of macropa-RPS-070. b) Distribution of ^{225}Ac-macropa-RPS-070 following intravenous injection in LNCaP tumor xenograft mice. Mice were sacrificed 4, 24, or 96 h post injection. Values for each time point are given as mean % ID g^{-1} ± 1 SEM.

In summary, we have identified macropa as an exceptional chelator for ^{225}Ac. This ligand completely complexes ^{225}Ac at a concentration that is two orders of magnitude lower than that at which DOTA can effectively radiolabel this α-emitter. Chelation is rapid as complexation of ^{225}Ac by macropa is complete after only 5 minutes at room temperature, whereas radiolabeling of DOTA only proceeds at 80 °C. Moreover, $[^{225}Ac(macropa)]^+$ is a highly inert complex that is at least as stable as $[^{225}Ac(DOTA)]^-$ in vitro and in vivo. A bifunctional

analogue of macropa was synthesized and successfully conjugated to two different types of vectors: a breast-cancer-targeting antibody, trastuzumab, and a prostate-cancer-targeting small molecule, RPS-070. Both macropa conjugates displayed rapid radiolabeling kinetics at room temperature, complexing more than 98% of the ^{225}Ac in under 20 minutes. ^{225}Ac-macropa-RPS-070 exhibited selective tumor uptake in a mouse xenograft model of prostate cancer. Notably, we did not observe accumulation of free ^{225}Ac in any organ over 4 days. Collectively, these results have significant implications for the use of ^{225}Ac in concert with antibodies and other protein constructs, which are unstable to temperatures greater than 37 °C and are susceptible to radiolysis when subject to either lengthy radiolabeling procedures or concentrated solutions of radionuclide. We anticipate that the implementation of macropa-NCS will further advance the clinical development of this important therapeutic radionuclide.

Supporting information for this article is given via a link at the end of the document. CCDC 1569019, 1569021 and 1569022 contain the supplementary crystallographic data for this paper. These data can be obtained free of charge from The Cambridge Crystallographic Data Centre.

Acknowledgements

This work was supported by Cornell University and by a Pilot Award from the Weill Cornell Medical College Clinical and Translational Science Center, funded by NIH/NCATS UL1TR00457. This research made use of the NMR Facility at Cornell University, which is supported in part by the NSF under award number CHE-1531632. TRIUMF receives funding via a contribution agreement with the National Research Council of Canada. We thank TRIUMF's ISAC facility for ion beam delivery and Drs. Peter Kunz and Jens Lassen for help with collecting ^{225}Ac and ^{225}Ra samples. We also thank Dr. Eszter Boros at Stony Brook University for providing us with trastuzumab, and Dr. J. David Warren of the Milstein Core Chemistry Facility at Weill Cornell Medicine for the use of equipment for analysis and purification.

Conflict of interest

The authors declare no conflict of interest.

Keywords: actinium · cancer · chelates · macrocycles · radiopharmaceuticals

How to cite: *Angew. Chem. Int. Ed.* **2017**, *56*, 14712–14717
Angew. Chem. **2017**, *129*, 14904–14909

[1] M. R. Harrison, T. Z. Wong, A. J. Armstrong, D. J. George, *Cancer Manag. Res.* **2013**, *5*, 1.
[2] R. Coleman, *Semin. Nucl. Med.* **2016**, *46*, 99.
[3] Y.-S. Kim, M. W. Brechbiel, *Tumor Biol.* **2012**, *33*, 573.
[4] Y. Dekempeneer, M. Keyaerts, A. Krasniqi, J. Puttemans, S. Muyldermans, T. Lahoutte, M. D'huyvetter, N. Devoogdt, *Expert Opin. Biol. Ther.* **2016**, *16*, 1035.
[5] E. W. Price, C. Orvig, *Chem. Soc. Rev.* **2014**, *43*, 260.
[6] M. W. Geerlings, F. M. Kaspersen, C. Apostolidis, R. van der Hout, *Nucl. Med. Commun.* **1993**, *14*, 121.
[7] M. R. McDevitt, D. Ma, L. T. Lai, J. Simon, P. Borchardt, R. K. Frank, K. Wu, V. Pellegrini, M. J. Curcio, M. Miederer, et al., *Science* **2001**, *294*, 1537.
[8] M. Miederer, D. A. Scheinberg, M. R. McDevitt, *Adv. Drug Delivery Rev.* **2008**, *60*, 1371.
[9] D. A. Scheinberg, M. R. McDevitt, *Curr. Radiopharm.* **2011**, *4*, 306.
[10] Memorial Sloan Kettering Cancer Center, Targeted Atomic Nano-Generators (Actinium-225-Labeled Humanized Anti-CD33 Monoclonal Antibody HuM195) in Patients With Advanced Myeloid Malignancies. ClinicalTrials.gov [website], Bethesda, MD: US National Library of Medicine. https://clinicaltrials.gov/ct2/show/NCT00672165. NLM identifier NCT00672165. Accessed Apr 20, **2017**.
[11] I. A. Davis, K. A. Glowienka, R. A. Boll, K. A. Deal, M. W. Brechbiel, M. Stabin, P. N. Bochsler, S. Mirzadeh, S. J. Kennel, *Nucl. Med. Biol.* **1999**, *26*, 581.
[12] K. A. Deal, I. A. Davis, S. Mirzadeh, S. J. Kennel, M. W. Brechbiel, *J. Med. Chem.* **1999**, *42*, 2988.
[13] L. L. Chappell, K. A. Deal, E. Dadachova, M. W. Brechbiel, *Bioconjugate Chem.* **2000**, *11*, 510.
[14] S. J. Kennel, L. L. Chappell, K. Dadachova, M. W. Brechbiel, T. K. Lankford, I. A. Davis, M. Stabin, S. Mirzadeh, *Cancer Biother. Radiopharm.* **2000**, *15*, 235.
[15] P. Comba, U. Jermilova, C. Orvig, B. O. Patrick, C. F. Ramogida, K. Rück, C. Schneider, M. Starke, *Chem. Eur. J.* **2017**, https://doi.org/10.1002/chem.201702284.
[16] M. R. McDevitt, D. Ma, J. Simon, R. K. Frank, D. A. Scheinberg, *Appl. Radiat. Isot.* **2002**, *57*, 841.
[17] A. E. Martell, R. M. Smith, *Critical Stability Constants Second Suppl.*, Springer, Boston, MA, **1989**, pp. 1–66.
[18] S. L. Wu, W. D. Horrocks, Jr., *J. Chem. Soc. Dalton Trans.* **1997**, 1497.
[19] R. D. Shannon, *Acta Crystallogr. Sect. A* **1976**, *32*, 751.
[20] M. Miederer, G. Henriksen, A. Alke, I. Mossbrugger, L. Quintanilla-Martinez, R. Senekowitsch-Schmidtke, M. Essler, *Clin. Cancer Res.* **2008**, *14*, 3555.
[21] M. Essler, F. C. Gärtner, F. Neff, B. Blechert, R. Senekowitsch-Schmidtke, F. Bruchertseifer, A. Morgenstern, C. Seidl, *Eur. J. Nucl. Med. Mol. Imaging* **2012**, *39*, 602.
[22] W. F. Maguire, M. R. McDevitt, P. M. Smith-Jones, D. A. Scheinberg, *J. Nucl. Med.* **2014**, *55*, 1492.
[23] M. Mato-Iglesias, A. Roca-Sabio, Z. Pálinkás, D. Esteban-Gómez, C. Platas-Iglesias, É. Tóth, A. de Blas, T. Rodríguez-Blas, *Inorg. Chem.* **2008**, *47*, 7840.
[24] A. Roca-Sabio, M. Mato-Iglesias, D. Esteban-Gómez, É. Tóth, A. de Blas, C. Platas-Iglesias, T. Rodríguez-Blas, *J. Am. Chem. Soc.* **2009**, *131*, 3331.
[25] R. Ferreirós-Martínez, D. Esteban-Gómez, É. Tóth, A. de Blas, C. Platas-Iglesias, T. Rodríguez-Blas, *Inorg. Chem.* **2011**, *50*, 3772.
[26] M. P. Jensen, R. Chiarizia, I. A. Shkrob, J. S. Ulicki, B. D. Spindler, D. J. Murphy, M. Hossain, A. Roca-Sabio, C. Platas-Iglesias, A. de Blas, et al., *Inorg. Chem.* **2014**, *53*, 6003.
[27] A. E. Martell, R. M. Smith, *Critical Stability Constants*, *Vol. 1*, Plenum, New York, **1974**.
[28] M. Regueiro-Figueroa, J. L. Barriada, A. Pallier, D. Esteban-Gómez, A. de Blas, T. Rodríguez-Blas, É. Tóth, C. Platas-Iglesias, *Inorg. Chem.* **2015**, *54*, 4940.
[29] M. G. Ferrier, E. R. Batista, J. M. Berg, E. R. Birnbaum, J. N. Cross, J. W. Engle, H. S. La Pierre, S. A. Kozimor, J. S. Lezama Pacheco, B. W. Stein, et al., *Nat. Commun.* **2016**, *7*, 12312.
[30] M. G. Ferrier, B. W. Stein, E. R. Batista, J. M. Berg, E. R. Birnbaum, J. W. Engle, K. D. John, S. A. Kozimor, J. S. Lezama Pacheco, L. N. Redman, *ACS Cent. Sci.* **2017**, *3*, 176.

[31] R. Ferreirós-Martínez, D. Esteban-Gómez, A. De Blas, C. Platas-Iglesias, T. Rodríguez-Blas, *Inorg. Chem.* **2009**, *48*, 11821.
[32] G. J. Beyer, R. Bergmann, K. Schomäcker, F. Rösch, G. Schäfer, E. V. Kulikov, A. F. Novgorodov, *Isot. Environ. Health Stud.* **1990**, *26*, 111.
[33] M. M. Moasser, *Oncogene* **2007**, *26*, 6469.
[34] B. Leyland-Jones, K. Gelmon, J.-P. Ayoub, A. Arnold, S. Verma, R. Dias, P. Ghahramani, *J. Clin. Oncol.* **2003**, *21*, 3965.
[35] D. Leveque, L. Gigou, J. P. Bergerat, *Curr. Clin. Pharmacol.* **2008**, *3*, 51.
[36] J. M. Kelly, A. Amor-Coarasa, A. Nikolopoulou, T. Wüstemann, P. Barelli, D. Kim, C. Williams, Jr., X. Zheng, C. Bi, B. Hu, et al., *J. Nucl. Med.* **2017**, *58*, 1442.
[37] A. P. Kozikowski, F. Nan, P. Conti, J. Zhang, E. Ramadan, T. Bzdega, B. Wroblewska, J. H. Neale, S. Pshenichkin, J. T. Wroblewski, *J. Med. Chem.* **2001**, *44*, 298.
[38] K. P. Maresca, S. M. Hillier, F. J. Femia, D. Keith, C. Barone, J. L. Joyal, C. N. Zimmerman, A. P. Kozikowski, J. A. Barrett, W. C. Eckelman, et al., *J. Med. Chem.* **2009**, *52*, 347.
[39] S. M. Hillier, K. P. Maresca, F. J. Femia, J. C. Marquis, C. A. Foss, N. Nguyen, C. N. Zimmerman, J. A. Barrett, W. C. Eckelman, M. G. Pomper, et al., *Cancer Res.* **2009**, *69*, 6932.
[40] J. A. Barrett, R. E. Coleman, S. J. Goldsmith, S. Vallabhajosula, N. A. Petry, S. Cho, T. Armor, J. B. Stubbs, K. P. Maresca, M. G. Stabin, et al., *J. Nucl. Med.* **2013**, *54*, 380.
[41] J. Kelly, A. Amor-Coarasa, A. Nikolopoulou, D. Kim, C. Williams, Jr., S. Ponnala, J. W. Babich, *Eur. J. Nucl. Med. Mol. Imaging* **2017**, *44*, 647.
[42] A. Ghosh, W. D. W. Heston, *J. Cell. Biochem.* **2004**, *91*, 528.
[43] M. S. Dennis, M. Zhang, Y. G. Meng, M. Kadkhodayan, D. Kirchhofer, D. Combs, L. A. Damico, *J. Biol. Chem.* **2002**, *277*, 35035.
[44] C. E. Dumelin, S. Trüssel, F. Buller, E. Trachsel, F. Bootz, Y. Zhang, L. Mannocci, S. C. Beck, M. Drumea-Mirancea, M. W. Seeliger, et al., *Angew. Chem. Int. Ed.* **2008**, *47*, 3196; *Angew. Chem.* **2008**, *120*, 3240.

Manuscript received: September 14, 2017
Accepted manuscript online: September 29, 2017
Version of record online: October 16, 2017

